Copper(I) *tert*-Butylthiolato Clusters as Single-Source Precursors for High-Quality Chalcocite Thin Films: Film Growth and Microstructure Control

Sven Schneider,[†,‡] John R. Ireland,[†] Mark C. Hersam,[†] and Tobin J. Marks*[,†]

Department of Chemistry, Materials Research Center, and Department of Materials Science and Engineering, Northwestern University, Evanston, Illinois 60208-3113, and Technische Universität München, Lichtenbergstrasse 4, 85747 Garching, Germany

Received January 7, 2007

Soluble cluster compounds of polymeric $(CuS^tBu)_\infty$ (**1**), such as the trialkylphosphine adducts $[(CuS^tBu)_4(PR_3)_2]$ (R = Me (**2a**), Et (**2b**)) or the mixed ligand cluster $Cu_7(S^tBu)_4(hfa)_3(PMe_3)_3$ (**3**, hfa = $CH(COCF_3)_2$), can be used as *single-source* precursors for chalcocite (α-Cu_2S) film growth. Toluene or tetrahydrofuran solutions of **2a**, **2b**, or **3** afford high-quality chalcocite thin films on glass by aerosol-assisted chemical vapor deposition (AACVD). The films were characterized by X-ray diffraction, X-ray photoelectron spectroscopy, optical spectroscopy, and Hall effect electrical measurements. Surface morphologies were analyzed by scanning electron microscopy and atomic force microscopy. Phase-pure Cu_2S films grown with **2a**/**b** consist of large micrometer-scale plates, which lie flat on the substrate surface, resulting in an extraordinarily strong $\langle 00l \rangle$ preferential orientation with respect to the hexagonal *high*-chalcocite substructure. The film morphologies as grown with precursor **3** suggest competing diketonate versus thiolate coordination at the {100} growth sites offering ligand-assisted film microstructural growth control.

Introduction

Among the sizable number of known Cu_xS polymorphs,[1] chalcocite (α-Cu_2S), which exhibits the lowest conductivity and highest optical absorption coefficient, is the most interesting polymorph for photovoltaic (PV) applications.[2] Not surprisingly, the use of chalcocite for PVs dates back to 1954.[3] Interest in the extensively studied CdS/Cu_2S heterojunction cells, which are typically prepared by topotactical Cu^+ for Cd^{2+} ion exchange on CdS surfaces, later declined because of their intrinsic interfacial instability, which is caused by diffusion of Cu^+ ions into the CdS layer.[4] Instead, ternary cuprous chalcogenide chalcopyrite materials ($CuME_2$; M = Ga, In; E = S, Se) are widely employed as absorbers in thin film solar cells.[5] However, much cheaper cuprous sulfide has recently been shown to afford stable *p*/*n* heterojunctions with *n*-type semiconductors other than CdS, such as TiO_2 and ZnO.[4,6] Furthermore, chalcocite has been utilized in other semiconductor devices such as nanoscale Cu_2S/Cu diodes.[7] As cation exchange is not possible for the production of such devices, gas-phase deposition techniques, which are not available for the growth of phase-pure α-Cu_2S thin films, would be highly desirable.[8]

Thiols have been used as the sulfur source for Cu_2S nanoparticle preparation,[9] and mixed metal copper(I) thiolates have been successfully employed as *single-source* precursors for chalcopyrite ($CuMS_2$, M = Ga, In) thin films and nanoparticles.[10] However, effective cuprous thiolate *single-source* precursors for the growth of copper-rich chalcocite (α-Cu_2S) thin films have proven elusive. We recently showed

[†] Northwestern University.
[‡] Technische Universität München.

(1) Chakrabarti, D. J.; Laughlin, D. E. In *Phase Diagrams of Binary Copper Alloys*; Subramanian, P. R.; Chakrabarti, D. J.; Laughlin, D. E., Eds.; ASM: Materials Park, OH, 1994.
(2) Nair, M. T. S.; Guerrero, L.; Nair, P. K. *Semicond. Sci. Technol.* **1998**, *13*, 1164.
(3) Reynolds, D. C.; Leies, G.; Antes, L. T.; Marburger, R. E. *Phys. Rev.* **1954**, *96*, 533.
(4) Reijnen, L.; Meester, B.; Goossens, A.; Schoonman, J. *Chem. Vap. Deposition* **2003**, *9*, 15.
(5) Goetzberger, A.; Hebling, C.; Schock, H.-W. *Mater. Sci. Eng. R* **2003**, *40*, 1.
(6) (a) Burgelman, M.; Pauwels, H. J. *Electron. Lett.* **1981**, *17*, 224. (b) Reijnen, L.; Meester, B.; Goossens, A.; Schoonman, J. *Mater. Sci. Eng.* **2002**, *C19*, 311. (c) Liu, G.; Schulmeyer, T.; Thissen, A.; A. Klein; Jaegermann, W. *Appl. Phys. Lett.* **2003**, *82*, 2269. (d) Boyle, D. S.; Govender, K.; O'Brien, P. *Thin Solid Films* **2003**, *431*, 483. (e) Berhanu, D.; Boyle, D. S.; Govender, K.; O'Brien, P. *J. Mater. Sci.: Mater. Electron.* **2003**, *14*, 579. (f) Reijnen, L.; Meester, B.; de Lange, F.; Schoonman, J.; Goosens, A. *Chem. Mater.* **2005**, *17*, 2724. (g) Reijnen, L.; Meester, B.; Goosens, A.; Schoonman, J. *Chem. Mater.* **2005**, *17*, 4142.
(7) Sakamoto, T.; Sunamura, H.; Kawaura, H.; Hasegawa, T.; Nakayama, T.; Aono, M. *Appl. Phys. Lett.* **2003**, *82*, 3032.
(8) Pfisterer, F. *Thin Solid Films* **2003**, *431*, 470.
(9) (a) Larsen, T. H.; Sigman, M.; Ghezelbash, A.; Doty, R. C.; Korgel, B. A. *J. Am. Chem. Soc.* **2003**, *125*, 5638. (b) Sigman, M. B., Jr.; Ghezelbash, A.; Hanrath, T.; Saunders, A. E.; Lee, F.; Korgel, B. A. *J. Am. Chem. Soc.* **2003**, *125*, 16050. (c) Chen, L.; Chen, Y.-B.; Wu, L.-M. *J. Am. Chem. Soc.* **2004**, *126*, 16334. (d) Kuzuya, T.; Tai, Y.; Yamamuro, S.; Sumiyama, K. *Sci. Technol. Adv. Mater.* **2005**, *6*, 84.
(10) (a) Hirpo, W.; Dhingra, S.; Sutorik, A. C.; Kanatzidis, M. G. *J. Am. Chem. Soc.* **1993**, *115*, 1597. (b) Hollingsworth, J. A.; Hepp, A. F.; Buhro, W. E. *Chem. Vap. Depos.* **1999**, *5*, 105. (c) Banger, K. K.; Cowen, J.; Hepp, A. F. *Chem. Mater.* **2001**, *13*, 3827. (d) Banger, K. K.; Harris, J. D.; Cowen, J. E.; Hepp, A. F. *Thin Solid Films* **2002**, *403*−*404*, 390. (e) Hollingsworth, J. A.; Banger, K. K.; Jin, M. H.-C.; Harris, J. D.; Cowen, J. E.; Bohannan, E. W.; Switzer, J. A.; Buhro, W. E.; Hepp, A. F. *Thin Solid Films* **2003**, *431*−*432*, 63. (f) Castro, S. L.; Bailey, S. G.; Raffaelle, R. P.; Banger, K. K.; Hepp, A. F. *Chem. Mater.* **2003**, *15*, 3142. (g) Castro, S. L.; Bailey, S. G.; Raffaelle, R. P.; Banger, K. K.; Hepp, A. F. *J. Phys. Chem. B* **2004**, *108*, 12429.

10.1021/cm0700495 CCC: $37.00
Published on Web 04/25/2007

that polymeric copper(I) thiolate $(CuS^tBu)_\infty$, which is insufficiently volatile to be useful as precursor for low-pressure chemical vapor deposition (LP-CVD), is readily soluble in organic solvents as the trialkylposphine adduct $(CuS^tBu)_4(PR_3)_2$ (R = Me (**2a**), Et (**2b**)).[11,12] Thermal characterization and preliminary film growth experiments with **2a** suggested this new *single-source* precursor class to be ideal for α-Cu_2S growth with liquid precursor delivery techniques, such as aerosol-assisted chemical vapor deposition (AACVD). We further reported copper(I) mixed ligand thiolato hexafluoroacetylacetonato (hfa^-) clusters, for example, $Cu_7(S^tBu)_4(hfa)_3(PMe_3)_3$ (**3**), as potential Cu_2S *single-source* precursors and showed that the thermolysis pathways of this cluster can be controlled by the interplay of C−S bond activating Lewis acid and C−S stabilizing Lewis base cluster building blocks.[13] In the present contribution we report an in-depth examination of high-quality chalcocite AACVD thin film growth using *single-source* precursors **2a**, **2b**, and **3**, particularly with respect to ligand-derived film microstructure control.

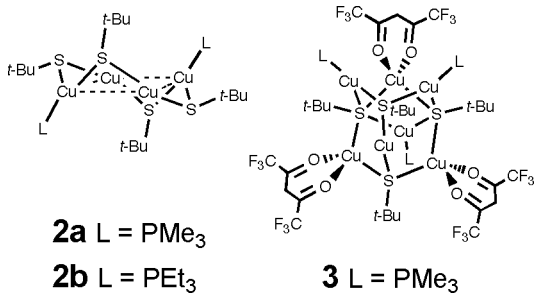

Experimental Section

Materials and Methods. $(CuS^tBu)_4(PMe_3)_2$ (**2a**), $(CuS^tBu)_4(PEt_3)_2$ (**2b**), and $Cu_7(S^tBu)_4(hfa)_3(PMe_3)_3$ (**3**) were synthesized as described earlier.[11−13] THF was distilled from sodium benzophenone ketyl immediately before use. Toluene was dried and deoxygenated by passing through columns packed with activated molecular sieves and Q5, respectively.

Thin Film Growth. Thin films of Cu_2S were grown on 2.5 × 2.5 cm glass slides using a horizontal cold-wall quartz reactor connected with a TSI 3076 Collison-type nebulizer via ∼25 cm 1/2 inch stainless steel tubing. Before deposition, the aerosol was conveyed through a preheating zone to facilitate solvent evaporation and phosphine cleavage prior to deposition. The reactor was evacuated and backfilled with argon three times prior to each film growth experiment, and the precursor reservoir was loaded via filter cannula (Whatman GF/B glass fiber filters) with freshly prepared solutions of **2a**, **2b**, or **3** in toluene (0.02−0.05 mol/L in Cu) or THF (0.03 mol/L in Cu), respectively. Cu_2S thin films were deposited on glass substrates (Corning 1737F), which had been cleaned with piranha solution and deionized water, and then degreased by ultrasonication with isopropanol and acetone. Substrates were placed on a graphite susceptor in the reactor and heated by an infrared lamp (Research, Inc., Minneapolis, MN). The chalcocite films were grown in situ with a susceptor temperature of 270−300 °C (**2a/b**) or 200−300 °C (**3**) and an argon flow rate of 1.5 L/min at atmospheric pressure (740−760 Torr).

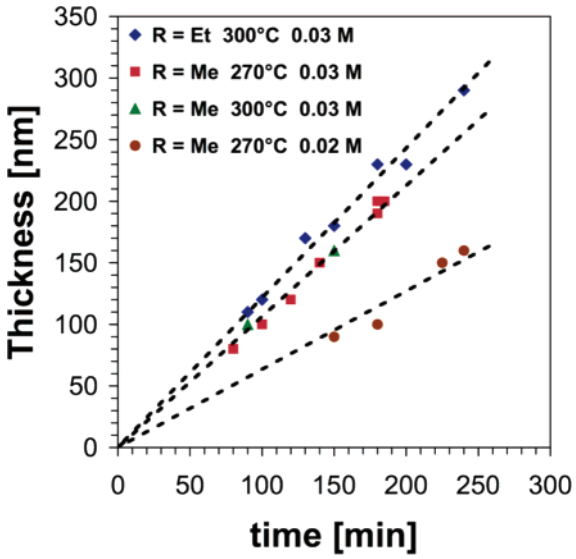

Figure 1. AACVD growth rates of Cu_2S thin films using *single-source* $(CuS^tBu)_4(PR_3)_2$ (R = Me (**2a**), R = Et (**2b**)) precursors in toluene at the indicated copper concentrations and susceptor temperatures.

Analytical Methods. Film thicknesses were measured with a Tencor P-10 profilometer after scribing the films with a razor blade. Film chemical compositions were examined with an Omicron ESCA probe X-ray photoelectron spectrometer. Film microstructures and surface morphologies were assessed with a Hitachi S4500 FE scanning electron microscope and a Digital Instruments Nanoscope III atomic force microscope operating in the contact mode. Phase purity and preferential growth orientations of the Cu_2S films were determined using $\theta-2\theta$ and ω scans. The $\theta-2\theta$ data were acquired with a computer-interfaced Rigaku DMAX-A powder diffractometer using Ni-filtered Cu Kα radiation. The ω-rocking curves were acquired on a home-built four-circle diffractometer with detector selected Cu Kα radiation.

Results

Cu_2S thin films were grown by AACVD using solutions of precursors **2a**, **2b**, or **3** in toluene and of **2a** in tetrahydrofuran (THF). Although we find that solvent identity has no detectable influence on the microstructural, chemical, optical, or electrical properties of the films, toluene is preferred as a result of the higher boiling point, thereby affording more stable growth rates. Likewise, evaporation of the solvent prior to deposition by maintaining the steel tubing for aerosol delivery at temperatures up to 150 °C does not affect the growth results. Brown, specular Cu_2S films that are adherent by the "Scotch-tape" test can be obtained with precursors **2a**/**b** at substrate temperatures between 250 and 300 °C. Below 250 °C, films are poorly adherent and not phase-pure, while at temperatures above 350 °C, no films are obtained, presumably because of premature gas-phase decomposition of the precursor. The growth rates with 0.03 mol/L (in Cu) toluene solutions are around 1.0−1.2 nm/min between 270 and 300 °C, with the rate for **2b** slightly greater than that for **2a** (Figure 1). We have recently shown that the Lewis acidic cluster building block Cu(hfa) in complex **3** facilitates C−S bond activation at significantly lower temperatures.[13] Consequently, Cu_2S can be grown over a wider

(11) Schneider, S.; Yang, Y.; Marks, T. J. *Chem. Mater.* **2005**, *17*, 4286.
(12) Schneider, S.; Dzudza, A; Raudaschl-Sieber, G.; Marks, T. J. *Chem. Mater.* **2007**, *19*, 2768.
(13) Schneider, S.; Roberts, J. A. S.; Salata, M. R.; Marks, T. J. *Angew. Chem., Int. Ed.* **2006**, *45*, 1733.

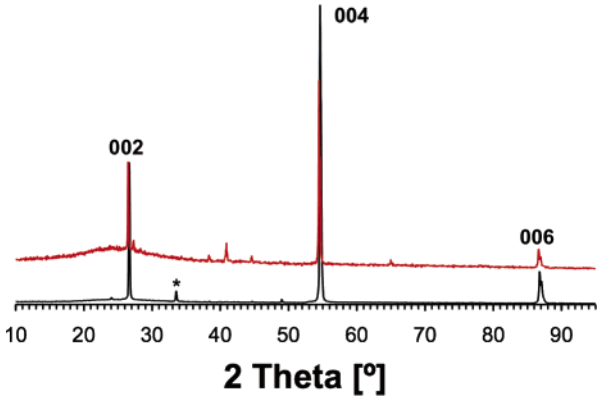

Figure 2. $\theta-2\theta$ XRD patterns (Cu Kα, 1.541 Å) of chalcocite films deposited by AACVD on glass from toluene solutions of **2b** (black, 300 °C) and **3** (red, 200 °C) with peak assignments referenced to hexagonal β-Cu_2S (JCPDS 26-1116). The asterisk indicates the [1000] reflection of a trace djurleite impurity.

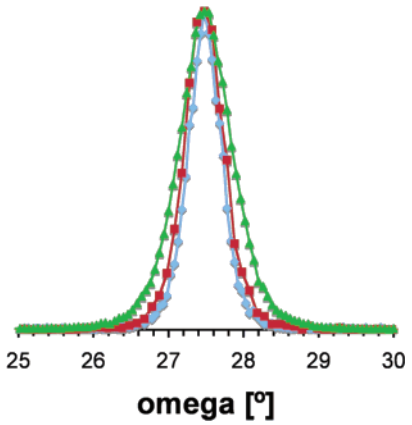

Figure 3. (004) reflection ω-scan rocking curves of Cu_2S films grown by AACVD on glass with precursors **2a** (270 °C, red), **2b** (300 °C, blue), and **3** (300 °C, green). Peaks heights are normalized to the green curve.

temperature range between 200 and 300 °C with precursor **3**.

The phase purity and crystallographic orientation of the present Cu_2S films were examined by X-ray diffraction (XRD). Films grown with precursor **2b** can be indexed in the β-Cu_2S (*high*-chalcocite, JCPDS 26-1116) lattice, as reported earlier for precursor **2a** (Figure 2).[11] However, hexagonal β-Cu_2S, which is the stable high-temperature chalcocite phase under the present growth conditions, is known to undergo a reversible phase transition at ~100 °C to a monoclinic α-Cu_2S (*low*-chalcocite, JCPDS 33-0490) superstructure.[14] The reflection indexing here indicates a very high $\langle 00l \rangle$ preferential orientation referenced to the β-Cu_2S lattice, with the (002) β-Cu_2S crystal plane transforming to the $(\bar{2}04)$ plane of the α-Cu_2S lattice. ω-Scan rocking curve analyses of 120−320 nm thin films grown with **2a** and **2b** at 270−300 °C confirm the extraordinarily high out-of-plane orientation on glass with a full width at half-maximum (fwhm) ~ 0.6° (Figure 3), while preferred in-plane orientation by φ scans could not be detected. The same preferred orientation with respect to the substrate surface was also found for reactively sputtered chalcocite thin films and

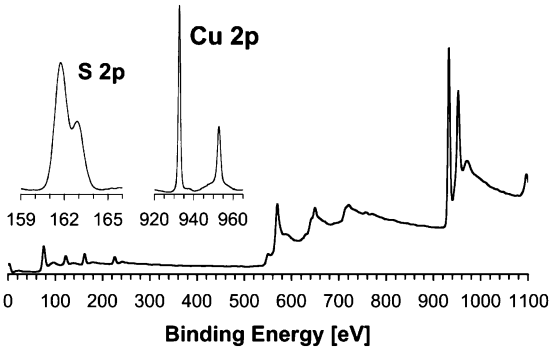

Figure 4. XPS spectrum of a 320 nm Cu_2S film grown by AACVD at 270 °C using precursor **2a** (15 min of Ar^+ sputtering/~45 Å). Insets: High-resolution scans of the Cu 2p and S 2p peaks.

monoclinic Cu_2S nanowires grown on Cu foil.[15,16] α-Cu_2S thin films with this crystallographic orientation cannot be easily distinguished from β-Cu_2S. However, powder XRD scans of a film detached by ultrasonication in acetone exhibit the additional reflections of α-Cu_2S.

Very thin Cu_2S films with thicknesses < 150 nm grown with either precursors **2a** or **2b** exhibit a small feature at $2\theta = 33.4°$, as shown in a typical $\theta-2\theta$ scan (Figure 2). The reflection is assigned to a trace impurity of the more copper-deficient cuprous sulfide polymorph djurleite (JCPDS 83-1463), another low temperature form of β-Cu_2S.[17] No reflections assignable to Cu metal impurities are found in the XRD patterns, even upon addition of 0.5 equiv of PR_3 (R = Me (**2a**), Et (**2b**)) per CuS^tBu unit to the precursor solutions in toluene or THF.

As with the homoleptic thiolates, cuprous sulfide films grown from toluene solutions (0.03 M in Cu) of mixed thiolate diketonate precursor **3** at temperatures of 200−300 °C consist of phase-pure α-Cu_2S by XRD. Likewise, films grown with precursors **2a**/**b** at 300 °C exhibit only diffraction features assignable to the β-Cu_2S (002), (004), and (006) planes, accounting for the high film texture, which is further supported by the (004) peak rocking curve, exhibiting a fwhm of 0.8° (Figure 3). However, thin films grown at 200 °C, which is too low a temperature to yield Cu_2S films with precursors **2a**/**b**, feature several additional weak reflections which can be assigned to other α-Cu_2S lattice planes, indicating reduced preferred crystallographic orientation (Figure 2). Accordingly, the ω-scan of the (004) reflection shows a very broad peak with a fwhm of ~15°. Despite the different Cu/S ratio in precursor **3** compared with **2a**/**b**, no diffraction features assignable to elemental copper or copper-deficient cuprous sulfide phases such as djurleite are found in any of the thin films.

X-ray photoelectron spectroscopy (XPS) of the present Cu_2S films supports the clean thermolysis of both homoleptic

(14) (a) Leon, M.; Terao, N.; Rueda, F. *Phys. Status Solidi* **1981**, *67*, K11. (b) Leon, M. *J. Mater. Sci.* **1990**, *25*, 669.

(15) (a) Armantrout, G. A.; Miller, D. E.; Vindelov, K. E.; Brown, T. G. *J. Vac. Sci.* **1979**, *16*, 212. (b) Vanhoecke, E.; Burgelman, M. *Thin Solid Films* **1984**, *112*, 97. (c) He Y. B.; Polity, A.; Österreicher, I.; Pfisterer, D.; Gregor, R.; Meyer, B. K.; Hardt, M. *Physica B* **2001**, *308*−*310*, 1069.

(16) Wang, S.; Yang, S.; Dai, Z. R.; Wang, Z. L. *Phys. Chem. Chem. Phys.* **2001**, *3*, 3750.

(17) Upon undergoing a phase transition from β-Cu_2S to pseudoorthorhombic djurleite, the 00*l* planes transform to *h*00. Therefore, the peak was assigned to the [1000] lattice planes, which were found in a simulated diffractogram at $2\theta = 33.28°$.

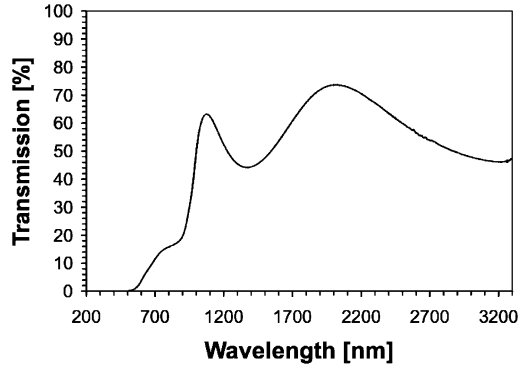

Figure 5. Transmission optical spectrum of a 320 nm Cu_2S film on glass grown with precursor **2a** at 270 °C.

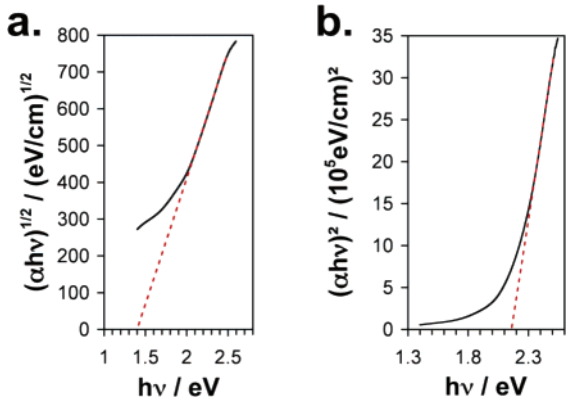

Figure 6. Estimates of indirect (a) and direct (b) Cu_2S bandgaps by plotting $(\alpha h\nu)^{1/2}$ and $(\alpha h\nu)^2$ vs $h\nu$, respectively.

thiolates **2a**/**b** and mixed thiolate β-diketonate precursor **3**. No features assignable to C, O, F, or P impurities are detected in the spectra after sputtering off a thin upper layer of about 45 Å (Figure 4). Photoelectron energy values for S ($2p_{3/2}$, 161.8 eV; $2p_{1/2}$, 163.0 eV; 2s, 228 eV) and Cu (3d, 4 eV; 3p, 77 eV; 3s, 125 eV; $2p_{3/2}$, 932.8 eV; $2p_{1/2}$, 953.1 eV) are in agreement with the literature.[18] The absence of copper(II) satellites further verifies the formation of the copper-rich chalcocite phase. Before sputtering, the films exhibit traces of oxygen and copper(II) features due to surface oxidation of the air-sensitive Cu_2S.

Transmission optical spectroscopy of a 320 nm Cu_2S film grown with precursor **2a** reveals transmission of less than 20% in the visible range and a cutoff at wavelengths lower than ~520 nm for incident light parallel to the film normal (Figure 5). Indirect (1.4 eV) and direct (2.2 eV) bandgaps were estimated from $(\alpha h\nu)^{1/2}$ and $(\alpha h\nu)^2$ vs $h\nu$ plots, respectively, and lie in an ideal range for PV applications (Figure 6). Mulder reported the single-crystal optical properties of the copper-rich Cu_xS polymorphs.[19] Accordingly, the results for our highly textured films are in excellent agreement with the optical properties of single-crystalline chalcocite in the direction of the crystallographic *c*-axis, with respect to the hexagonal sulfur lattice.

The Cu_2S film electrical properties were characterized by four-probe and Hall effect measurements at room temperature. Films grown with precursors **2a**/**b** exhibit conductivities of 15−55 S/cm. Hall carrier mobilities for 120−320 nm films grown with both precursors at 270−300 °C are relatively constant at around 2.6(8) $cm^2/(V\ s)$. All films exhibit heavy *p*-type doping with carrier concentrations (hole) around 10^{20} cm^{-3}, similar to results reported for RF sputtered α-Cu_2S films.[15c,20] Postdeposition annealing of a 200 nm film grown with **2a** up to 350 °C (2.5 h) at atmospheric pressure under a flow of forming gas (5% H_2 in N_2) did not detectably alter the electrical properties, hence, the Cu_xS stoichiometry. Wagner and Wiemhöfer have shown that the Cu vacancies in Cu_xS act as acceptors at the valence band edge with very high ionization probabilities.[20b] Therefore, the present films are in the $Cu_{1.999}S$−$Cu_{1.992}S$ compositional range with a slight dependence of the Cu_xS stoichiometry on the film thickness (Figure 7). The lower end of this Cu/S stoichiometry is at the edge of the reported chalcocite homogeneity range (Cu_xS, $x = 2.000 \pm 0.002$ to 1.993 ± 0.002), which is in agreement with the present observation of trace copper-deficient djurleite ($x = 1.965$−1.934) impurities in films < 150 nm thick by XRD (Figure 2).[1] Temperature-dependent conductivity measurements between room temperature and 77 K evidence a fall in resistivity with falling temperature for the semiconducting chalcocite thin films and are in excellent agreement

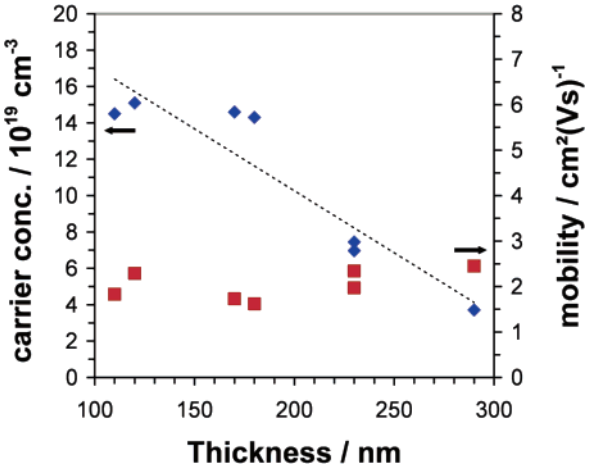

Figure 7. Carrier concentrations (blue) and hole mobilities (red) from Hall effect measurements as a function of film thickness for Cu_2S thin films grown with precursor **2b** at 300 °C.

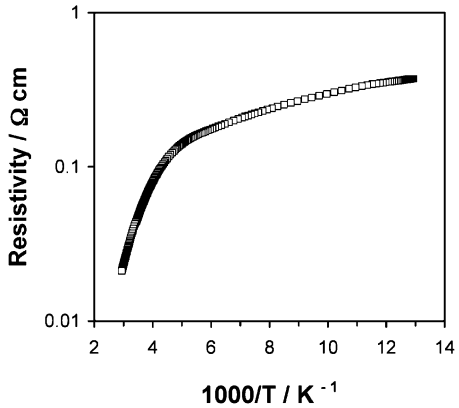

Figure 8. Temperature dependence of the four-probe resistivity of a 230 nm Cu_2S thin film grown with precursor **2b** at 300 °C.

(18) Bhide, V. G.; Salkalachen, S.; Rastogi, A. C.; Rao, C. N. R.; Hedge, M. S. *J. Phys. D: Appl. Phys.* **1981**, *14*, 1647.
(19) (a) Mulder, B. J. *Phys. Status Solidi* **1972**, *13*, 79. (b) Mulder, B. J. *Phys. Status Solidi* **1973**, *15*, 409. (c) Mulder, B. J. *Phys. Status Solidi* **1973**, *18*, 633.
(20) (a) Leong, J. Y.; Yee, J. H. *Appl. Phys. Lett.* **1979**, *35*, 601. (b) Wagner, R.; Wiemhöfer, H.-D. *J. Phys. Chem. Solids* **1983**, *44*, 801.

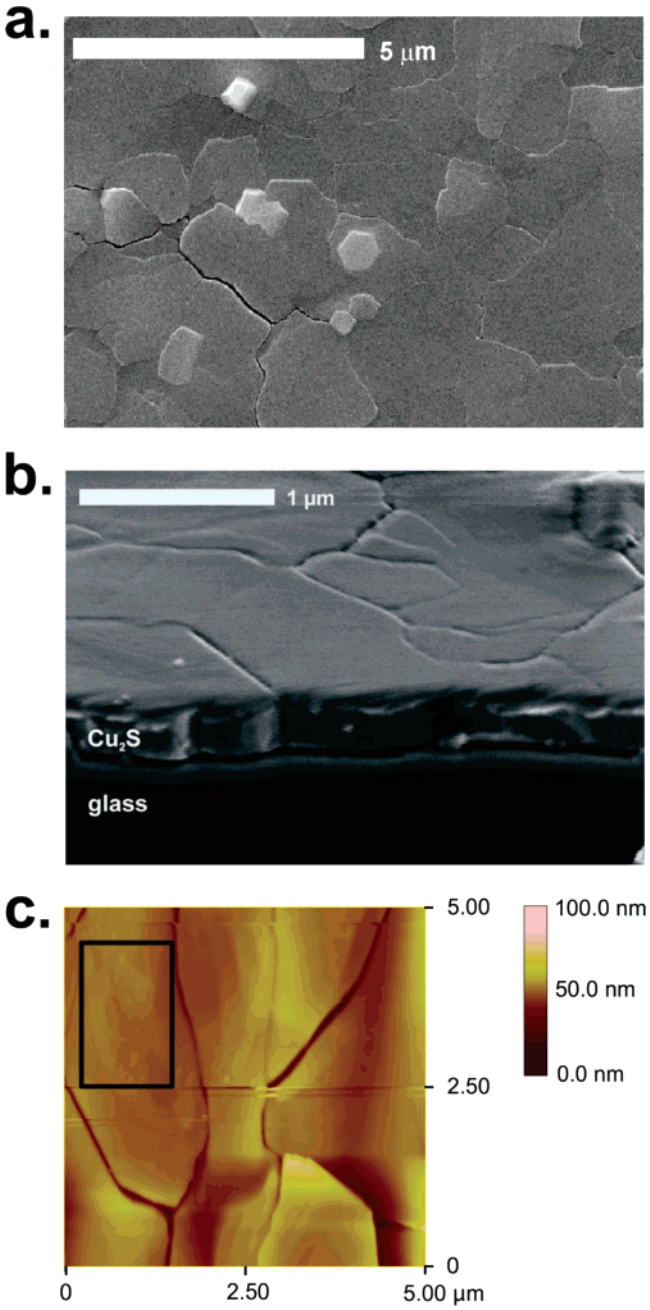

Figure 9. Typical micrographic images of α-Cu_2S films grown using precursor **2a** at 270−300 °C: a. Plan view SEM image. b. Cross-sectional SEM image. c. AFM image; the total rms roughness over 25 μm^2 is 6.1 nm. The single grain roughness of the area inscribed by the black box is ∼1.1 nm.

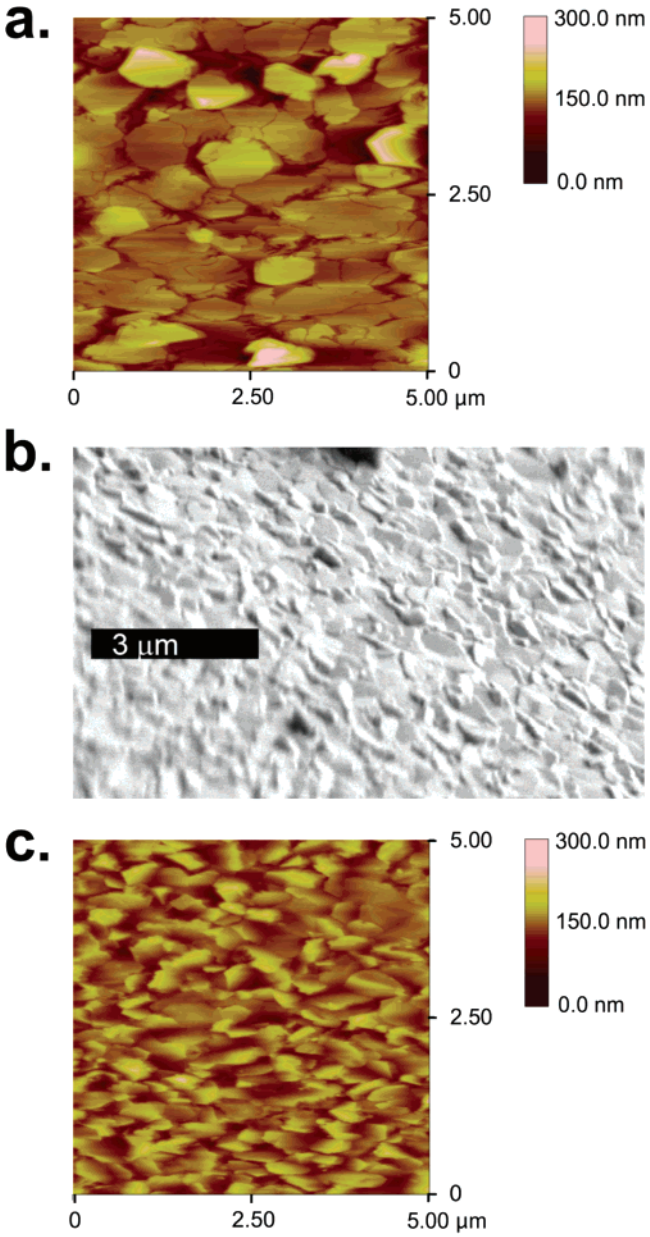

Figure 10. Typical micrographic images of α-Cu_2S on glass grown using precursor **3**: a. AFM image of a film grown at 300 °C; the total rms roughness over 25 μm^2 is 26 nm. b and c. Tilted angle SEM image (b) and AFM image (c) of a film grown at 200 °C; the total rms roughness over 25 μm^2 is 22 nm.

with literature observations (Figure 8).[15c] Films grown with precursor **3** exhibit identical electrical properties at room temperature with respect to average conductivity (27 S/cm), mobility (3 $cm^2/(V\ s)$), and hole concentration (5×10^{19} cm^{-3}), confirming the same Cu_xS stoichiometry range and the absence of the potential *n*-type dopant fluorine.

The morphologies of the present Cu_2S films were examined by scanning electron microscopy (SEM) and atomic force microscopy (AFM). The SEM images show that the Cu_2S films grown with precursors **2a**/**b** at 270−300 °C consist of large plates with in-plane dimensions in the ∼1−2 μm range and the grain boundaries perpendicular to the substrate surface (Figure 9). Overall, they exhibit a very smooth appearance and relatively featureless surfaces with few hexagonally shaped crystallites visible. AFM analysis confirms the smoothness of the microplatelets with a root mean square (rms) roughness over an area of 1−2 μm^2 of only 1−3 nm and an overall roughness over 25 μm^2 of about 5−10 nm. SEM and AFM images of typical films grown with precursor **3** at 200 and 300 °C are depicted in Figure 10. As for the homoleptic thiolato precursors, the microcrystalline Cu_2S films grown with precursor **3** at 300 °C are composed of large shingle-like plates, albeit with smaller dimensions, in the submicrometer range. Consequently, the rms surface roughness by AFM (∼20−25 nm) is considerably greater than for the Cu_2S films grown with **2a**/**b**. Likewise, films grown at 200 °C consist of nanosized plates with a rms roughness ∼ 20 nm. The SEM micrograph shows that the low-temperature growth yields crystallites which are slightly tilted with respect to the surface normal. This result

is in accord with the reduced preferred crystallographic orientation found by XRD.

Discussion

Thermal analysis suggests for trialkylphosphine adducts **2a** and **2b**, which are highly soluble in organic solvents, that multistep phosphine cleavage accompanies thermolysis at temperatures close to those of the parent complex **1**.[12] This thermal behavior renders the trialkylphosphine derivatives soluble sources of **1**, and therefore ideal *single-source* precursors for AACVD growth of chalcocite with good growth rates. These resulting films are phase-pure, with no observable signs of reduction to copper by the phosphine ligands and only traces of more copper-deficient djurleite at very thin film thicknesses. The observed thickness dependence of the overall Cu_xS stoichiometry implicates a layer with copper depletion upon initial film growth but cannot be unambiguously established with the data at hand. However, we believe that the thermolysis processes previously found in offline pyrolysis experiments[12] apply reasonably well to the present film growth leading to the same chalcocite phase. As pointed out previously, free radical processes could account for the *p*-type doping and djurleite traces.[12] Similar results as with **2a**/**b** were found with mixed thiolato diketonate precursor **3**. Furthermore, Lewis acid-assisted C−S activation in cluster **3** enables the growth of phase-pure α-Cu_2S films at temperatures as low as 200 °C.

Despite the moderate deposition temperatures, α-Cu_2S films grown above 250 °C are highly [00*l*]-oriented with respect to the pseudo-hexagonal sulfide sublattice, although the present deposition process is not strictly a vapor-phase growth method. Thus, films grown by spray pyrolysis are reported in the literature to often suffer from poor morphologies, including porosity and lack of preferred crystallographic orientation.[21] Characterization of the present precursor system has demonstrated the structural flexibility of the cuprous thiolates in the solid state, solution, and the gas-phase owing to the low coordination numbers of the metal centers.[12] This generally suggests a high mobility of the cluster building blocks at elevated temperatures on the substrate surface, most likely enabling the homogeneous growth and preferred crystallographic orientation of the high-quality Cu_2S films. In fact, the precursor melting points lie well below the thiolato ligand decomposition temperatures.

The film texture and morphology observed in this work suggest a very uniform film growth mechanism. Korgel and co-workers have examined the growth mechanism of Cu_2S nanoparticles from in situ generated Cu^I dodecanethiolate.[9a,b] The solventless growth conditions employed afford monodisperse nanodisks that exhibit hexagonal β-Cu_2S cell parameters with the [001] orientation normal to the plate faces. Preferred adsorption of the thiolate ligands on the six {100} planes due to their higher surface energies compared with (001) is proposed to limit [001] growth and cause the nanoparticle shape. The hexagonal disks with large (001) crystal facets then orient flat on the surface or stack together to form chain-like superstructures. This growth mechanism is most likely also applicable to Cu_2S thin film growth with precursors **2a**/**b**. The low melting point of CuS^tBu induces melting of the particles in the gas phase and/or on the substrate surface prior to decomposition, thereby delivering highly mobile CuS^tBu building blocks. Gas-phase C−S bond thermolysis seems highly unlikely at substrate temperatures close to the onset of C−S activation. The present high [00*l*] out-of-plane orientation without in-plane orientation of the films suggests nucleation of islands at several sites with random orientation of the hexagonal *a* and *b* axes on the amorphous substrate, which evolve into a continuous, dense film by preferred growth along their respective {100} surfaces. The stacking of such plate-like crystallites accounts for *c*-axis growth of the β-Cu_2S layered material, which is supported by residual hexagonal features remaining on the film surface (Figure 9, top). Introducing a further anionic ligand results in competition with thiolate for binding to the growth sites. Thus, Korgel isolated considerably smaller Cu_2S nanoparticles using octanoate capping ligands.[9b] Likewise, we find considerably smaller grain sizes for films grown with mixed ligand cluster **3**, which can be explained by competitive hfa^- coordination to growth sites, resulting in more nucleation sites. Accordingly, the overall film roughness is approximately two times that of films grown with **2a**/**b**. Even smaller grain sizes with precursor **3** at 200 °C finally lead to the observed reduced crystallographic orientation.

Conclusions

Copper thiolate clusters **2a**, **2b**, and **3** are excellent *single-source* precursors for the solution-based growth of phase-pure chalcocite as shown by AACVD growth of high quality α-Cu_2S thin films. Lewis acid-assisted C−S bond activation with precursor **3** enables growth temperatures as low as 200 °C. The structural flexibility of low-coordinate copper(I) in thiolato clusters is believed to account for highly mobile copper thiolate building blocks on the substrate surface thus responsible for the high Cu_2S film out-of-plane orientation even at low growth temperatures. This texture implicates a growth mechanism similar to that described for Cu_2S nanoparticles. Competitive hfa^- coordination at the growth sites using precursor **3** provides the possibility of ligand-assisted film microstructural control with only modestly reduced preferred orientation, evident from the generally smaller grain sizes. The electrical and optical properties as well as the smooth film morphologies make the α-Cu_2S films grown with **2a**, **2b**, and **3** promising components for optoelectronic applications.

Acknowledgment. We thank the NSF (CMS-0510895), the NSF MRSEC program (DMR-0076097), and NREL (XAT-5-33636-02) for financial support. S.S. thanks the DFG for a postdoctoral fellowship under the Emmy-Noether Programm.

CM0700495

(21) Kodas, T. T.; Hampden-Smith, M. *Aerosol Processing of Materials*; Wiley: New York, 1999.